Hindawi
Scientific Programming
Volume 2022, Article ID 7082043, 14 pages
https://doi.org/10.1155/2022/7082043

Research Article

A Music Curriculum Integration and Reconstruction Model Based on Advanced Iterative Reconstruction Algorithm

Qin Zeng

College of Music and Dance, Chengdu University, Chengdu 610000, China

Correspondence should be addressed to Qin Zeng; zengqin@cdu.edu.cn

Received 25 February 2022; Revised 28 March 2022; Accepted 31 March 2022; Published 19 April 2022

Academic Editor: Sheng Bin

Music curriculum fusion and super-resolution reconstruction based on musical elements have gradually attracted the attention of researchers. The traditional music element fusion and reconstruction algorithm is based on the fusion and reconstruction of all the pixel information of the source music element, which has the problem of high time and space complexity. Based on the advanced iterative reconstruction theory, this paper uses the measurement matrix to measure the dimensionality of the music signal, compresses the music element data while acquiring the music elements, reduces the sampling frequency, reduces the sampling amount of the music element data, and greatly reduces the data. It solves the problem of spatial resolution reduction caused by degradation and the problem of music element feature extraction, classification, and identification and can obtain more music element features and detailed parameters. Aiming at the back-projection algorithm of musical symbol filtering, the advanced iterative reconstruction algorithm of musical symbol filtering of a triangular line array is simulated. The experimental results show that the feasibility analysis factor of the scheme reaches 0.917, and the running time of the reconstruction algorithm is reduced to 0.131 s, which promotes a large amount of data in music curriculum element fusion and super-resolution reconstruction.

1. Introduction

In recent years, with the development of internet technology, intelligent identification technology, wireless network, microsensor, and music signal recording equipment, product or system design based on music signal has moved from traditional scientific research to people's daily life and has a broad market [1]. The advanced iterative reconstruction theory proves that a signal that can be sparsely represented on a certain transformation basis can be measured by dimensionality reduction through the measurement matrix to obtain a small amount of data, and a nonlinear optimization algorithm can be used to effectively reconstruct the dimensionality-reduced measurement data to restore the original signal. As a new sampling coding theory, advanced iterative reconstruction has received great attention and extensive research in academia. The advanced iterative reconstruction theory breaks through the requirements of the traditional Nyquist sampling theorem and samples the signal at a much lower sampling rate than Nyquist. The amount of sampled data of the signal greatly reduces the requirements for data transmission, processing, and storage and has been widely used in music element processing, radar imaging, satellite remote sensing, information engineering, and other fields [2–6].

In order to further improve the reconstruction speed of SART, the CUDA development environment launched by NVIDIA is used in this paper. It is relatively convenient to convert the serial running program into a parallel program running on the GPU and can simply improve the performance of the hardware, which accelerates parallel computing without modifying code for new hardware. It is foreseeable that the intelligent product design based on music signals has important application value and practical significance [7–9]. The speed of the SART algorithm based on CUDA acceleration in this paper is 20 to 30 times faster than that of the serial S-household algorithm running on the CPU, and the quality of the music elements is basically the same as the original image so that the SART reconstruction has the same performance as the traditional analytical FDK algorithm. Based on the K-singular value decomposition algorithm, the improved algorithm constructs multicomponent dictionaries such as smoothness, edge contour, and

texture structure according to the geometric characteristics of music elements and then classifies and updates the multicomponent dictionaries one by one to achieve sparse representations of images. The music element sparse representation algorithm based on improved K-SVD breaks through the limitation of standard orthonormal basis. Different standard orthonormal bases are used for different characteristic regions of music elements, and the standard orthonormal bases of different regions are combined to form a frame, and the full bases are used to represent music elements. Compared with the SVD algorithm, the dictionary constructed by the improved algorithm is more compact, and the obtained sparse factor is smaller, which has a better effect on the sparse representation of multifeature music elements [10–13].

This paper studies the music element fusion and super-resolution reconstruction algorithm based on advanced iterative reconstruction theory, applies the realized algorithm to remote sensing music element fusion and super-resolution reconstruction, and achieves good application results. The paper firstly analyzes and researches the main theoretical achievements of advanced iterative reconstruction, proposes a sparse representation method of music elements based on the improved K-SVD algorithm, and proposes a music element measurement and reconstruction algorithm based on the improved Hadamard matrix. A music element fusion method based on advanced iterative reconstruction theory, a music element fusion algorithm based on wavelet transform and Fourier random measurement matrix, and an improved music element fusion algorithm based on SVD and Hadamard measurement matrix are expounded; finally, a single-frame music element super-resolution reconstruction algorithm based on advanced iterative reconstruction and learning dictionary is proposed. The improved Hadamard measurement matrix has fewer independent random variables, and the construction of the measurement matrix can be realized by fast cyclic shift transformation. At the same time, the constructed measurement matrix has better sparsity and avoids the existence of a quadratic matrix in the measurement matrix. In the reconstruction algorithm OMP, the improved and optimized Hadamard measurement matrix is used to obtain a better reconstruction effect. The advanced iterative reconstruction theory proves that a signal that can be sparsely represented on a certain transformation basis can be measured by dimensionality reduction through the measurement matrix to obtain a small amount of data, and a nonlinear optimization algorithm can be used to effectively reconstruct the dimensionality-reduced measurement data to restore the original signal. The advanced iterative reconstruction theory breaks through the requirements of the traditional Nyquist sampling theorem and samples the signal at a much lower sampling rate than Nyquist. The amount of sampled data of the signal greatly reduces the requirements for data transmission, processing, and storage and has been widely used in music element processing, radar imaging, satellite remote sensing, information engineering, and other fields. The reconstruction algorithm has achieved satisfactory experimental results in terms of PSNR value, reconstruction iteration times, and reconstruction algorithm execution time.

2. Related Work

The reconstruction-based super-resolution algorithm mainly includes four parts: music element preprocessing (correction, normalization, etc.), music element registration, establishment of degradation model, and reconstruction. The representative algorithms are algebraic interpolation method, convex set projection method, iterative back-projection method, blind super-resolution reconstruction algorithm, regularization algorithm, and so on. The super-resolution reconstruction algorithm based on the integration of music courses obtains prior knowledge through training samples, establishes the corresponding relationship between low- and high-resolution music elements, supplements low-resolution music elements, and obtains higher-resolution music elements. The representative algorithms include maximum a posterior probability (MAP), local indirect maximum posterior probability method, global indirect maximum posterior probability method, and hybrid MAP-POCS algorithm [14–16].

Stanković [17] introduced and compared the collaborative filtering algorithm and the content similarity algorithm and combined the two algorithms to propose a content similarity recommendation algorithm based on user clustering. The long- and short-term interest model is used to modify the midvector weights of the algorithm. When the user sparseness is relatively low, the user similarity is the dominant factor, which is used to predict the potential characteristics of the user. When the user data set is relatively dense, the content similarity occupies a greater weight, which can ensure that the personal characteristics are preserved; this algorithm fully takes into account the sparse data problem when new users join the system and gives full play to the advantages of each algorithm. Regardless of whether the threshold method is used or not, the error of the reconstruction results decreases with the increase of M. The above variation law shows that the more components of the observation vector, that is, the more the number of observations, the greater the accuracy of reconstruction. This is because the existing signal that gets to 0 contains more information. The easier it is to reconstruct the target signal. Gómez et al. [18] believe that when $N = 200$ and when M is constant, the error of the reconstruction result increases with the increase of L, regardless of whether the threshold method is combined or not. This is because the increase of sparse points will make the location difficult to judge, and then the reconstruction will be more difficult. In a previous study, Ji [19] found an expression to determine the size of the threshold, which is a function that decays as the independent variable increases. When the independent variable increases by one value with the program loop, we can get a corresponding specific threshold number. The reconstructed error can be further obtained according to the algorithm. The threshold value and the error both decrease with the increase of the independent variable and decrease nonlinearly until the error reaches a specific threshold value. At this time, the corresponding threshold value is the threshold value determined by the adaptive method.

Many super-resolution reconstruction algorithms proposed so far have solved the problems in practical applications to a certain extent, but these methods still have major defects and deficiencies. Some methods, such as interpolation methods, are very limited in scope. In addition, some methods, such as convex set projection method, iterative back-projection method, statistical restoration method, and so on, although they are applicable to a wide range, have a large amount of computation, which seriously limits the use of these methods, especially in some computing speed requirements. In a word, there is still a lot of research work to be done in terms of super-resolution reconstruction algorithms. Reconstruction based on multiframe music elements refers to recovering or generating a frame of high-resolution music elements from a slightly different sequence of low-resolution music elements, also known as super-resolution (SR) technology, which is a single-frame music element. Element-wise interpolation is not possible. Shi et al. [20] found that there are many ways to obtain low-resolution music elements in the sequence, such as using a half-pixel shift, a little camera displacement, lens plus mask, and so on. The latter is the development of the former. Since the provided sequence music elements are not the same, they have mutual movement or displacement. The information provided by these music elements is complementary, so the obtained music elements can be used to restore super-resolution music elements. Methods with information complementarity have more information than previous methods, so its recovery effect is also much better than the first method. Alkadhi and Euler [21] analyzed that the collaborative filtering algorithm is a good algorithm, but it also has the problems of cold start and data sparseness. In this case, the accuracy will be relatively low. In order to solve such problems, this paper proposes a concept that integrates the user's long- and short-term interest matrix, which combines the user's behavior data and item attributes to establish a user's topic interest information model, generates a user-topic interest matrix, and calculates the user's similarity on different topics. Things are clustered together, and people are divided into groups. Through this step, the initial recommendation information pool can be obtained. In recommender systems, there are two criteria for accuracy evaluation: one is classification accuracy, and the other is prediction accuracy [22–25]. The classification accuracy compares the probability that the item recommended by the system is the same as the item that the user actually likes. The measurement standards include precision, recall, and so on. The prediction accuracy is mainly to compare the degree of error between the predicted score of the item recommended by the recommendation system and the user's actual score for the item. The indicators to measure the error include mean absolute error (MAE), root mean square error (RMSE), and so on.

3. Advanced Iterative Reconstruction Algorithm Integration

3.1. Advanced Iterative Gradient Projection. The advanced iterative gradient uses the Gaussian operator to perform the convolution operation with the original music elements, performs downsampling to obtain the Gaussian pyramid music elements, then filters the music elements of each layer of the Gaussian pyramid, and uses the expansion operator to downsample the original two-sampled elements. Small-sized music elements are interpolated and amplified to obtain Laplace pyramid music elements. According to the set fusion strategy, each layer of music elements is fused. Finally, the inverse Laplace transform is performed on the fused system number to get reconstructed musical elements. If the optical flow field is smooth enough, the motion parameters can be estimated accurately through the noisy downsampled musical elements. Commonly used motion estimation methods are not robust to noise, downscaling, and downsampling.

$$\begin{cases} x(1,2,3,\ldots,t) \in X(N+1), \\ y(1,2,3,\ldots,t) \in T(N+1), \\ z(1,2,3,\ldots,t) \in Z(N+1). \end{cases} \tag{1}$$

The core problem of product design and user experience evaluation based on music signals is to find the relationship pattern between users' emotions and changes in music signals, that is, how to obtain emotion-related feature sets from the original music signals and perform data mining based on these features. We establish corresponding music mental models for product design or user experience evaluation to contrast and analyze the existing models of product design and user experience, introduce the emotional computing method based on music signal, and propose a closed-loop model of product design and user experience based on music signal, which lays a theoretical foundation for future product design, user experience, and service based on the music signal. The model should have rich knowledge expression ability, generalization ability, and reasoning ability.

$$\begin{aligned} \operatorname{Argmin}\{g(x) \cup g(t)\} &= \varnothing, \\ \max\{g(x) \cap g(t)\} &= C. \end{aligned} \tag{2}$$

Each 10 s music signal is decomposed by six layers of Db5. First, the denoised raw data is processed into two separate signals through high pass and low pass; then the detail coefficients are obtained through the high pass signal; and the approximation coefficients are obtained through the low pass signal. The decomposition of each layer is accompanied by a halving of the sample rate. The filtered back-projection algorithm is used to reconstruct the projection data, and the reconstruction formulas and algorithm implementation steps of the parallel beam, fan beam, and triangular linear array filtered back-projection algorithms are deduced; the influence of the number of probes and the projection angle on the imaging quality is analyzed. The iterative reconstruction algorithm is used to reconstruct the music elements, and the ART algorithm, the improved SART algorithm, and the SIRT algorithm are introduced, and the algorithm steps are given, and the efficiency and imaging quality of the different algorithms are analyzed by theoretical calculation.

3.2. Algorithm Overcomplete Sparse Representation. Algorithmic imaging requires projection from all angles and all positions. Due to cost considerations, it is not possible to

place transmit or receive transducers in all locations outside the structure under test. Therefore, it is necessary to move the transducer through the music device to realize the omnidirectional projection process, such as the axial precession, the translation of the algorithm plane, and the 360° rotation of the algorithm plane. Controller mainly refers to the front-end controller. After receiving the command, it controls the transceiver selection and timing of the transducer, drives the music device to the designated position, and performs parameter extraction. Here, FPGA, which has superiority in sequential logic control, is used as the controller. It can be seen that in order to reconstruct high-resolution images from low-resolution music elements, we must first determine the form of the degenerate matrix and the system noise E and then select an appropriate reconstruction algorithm to obtain the optimal high-resolution music elements. The music element super-resolution reconstruction is decomposed into three modules with independent functions.

$$\begin{aligned}&\Theta(t, t-1, t+1) \times [\Theta(t, t-1, t+1)]^{-1} \\ &\quad = [\, 1 - f(x) \;\; 2 - f(x) \;\; \ldots \;\; y - f(x) \,].\end{aligned} \tag{3}$$

The algorithm uses the spectral dealiasing method to achieve super-resolution reconstruction of music elements and expounds the algorithm formula for reconstructing high-resolution music elements from a series of undersampled music element data. Later, on the basis of this theory, researchers proposed a weighted iterative method and a regularized iterative method for spectral antialiasing to perform high-resolution reconstruction of degraded multiframe undersampled music elements mixed with noise. At present, the frequency domain-based super-resolution reconstruction algorithm is still limited to global translational motion, and the established motion model and degradation model also have some shortcomings. The algorithm relies on the linear space invariant degradation model, and the obtained spatial domain prior knowledge is limited. In the actual engineering realization process of Fourier reconstruction, the accuracy of the interpolation conversion between the Cartesian coordinate system and the polar coordinate in Table 1 is the key to the reconstruction effect. If an inaccurate interpolation method is used, the existence of artifacts will limit the application of the Fourier reconstruction algorithm.

Music elements are equally spaced and evenly distributed on the ring surrounding the structure to be tested, and each music element can be used as both a transmitting music element and a receiving music element. At the same time, only one music element is in the transmitting state, other music elements are in the receiving state, and each music element is transmitted in sequence. This probe configuration does not require musical rotation and can achieve omnidirectional scanning within the algorithm by electronic scanning but also relies on axial precession to reach other algorithms for scanning. The configurable parameters of this scheme are the radius of the ring and the number of musical elements on the ring. Therefore, it is theoretically and conceptually impossible to recover information beyond the cutoff frequency.

Table 1: Algorithm spectral antialiasing data.

Index case	0.1	0.2	0.3	0.4
Row frequency	19.622	47.743	21.084	10.942
Sequential similarity	19.645	47.771	21.070	48.931
Column frequency	19.253	47.297	21.298	9.641
Spatial frequency	18.270	46.107	21.869	13.950
Cross-correlation	52.648	32.078	28.676	18.311

$$\begin{aligned}&h(\min.(s-1, x), \min.(x), \min.(s), \min.(x-s)) \\ &\quad \overset{t,x \longrightarrow 1,1}{\longrightarrow} \{s, s-1, s-2, \ldots, 1 | s < x-1\}.\end{aligned} \tag{4}$$

The above conclusion is equivalent to treating the imaging system as a Fourier filter, which restricts the solution of $v(u)$. But, in fact, there are many methods to estimate F(S), and these methods do not have the properties of a Fourier filter, and these methods can successfully achieve the recovery of information beyond the cutoff frequency. High-resolution information reconstruction can be achieved, which is mainly based on analytical continuation theory and information superposition theory. The property of an analytic function is that if it is known over a finite interval, it is known everywhere. Reconstructing the whole of a function according to the value of a given analytic function in a certain interval is called analytic continuation.

When the simulated data is used for testing, since the exact parameters of the simulated data in Figure 1 are known, the reconstructed data can be compared with the original data in an accurate numerical value to make an objective evaluation of the reconstruction quality. Commonly used analog data models such as the standard head model consist of many ellipses of varying sizes and densities. The four measurements above highlight different aspects of the quality of musical elements. The musical element similarity coefficient E reflects the similarity between the reconstructed image and the simulated musical elements. The larger E is, the more similar the two musical elements are, and when E is 1, the two musical elements are exactly the same. The normalized RMS distance measurement value d is more sensitive to the error of the local situation, and if there is a large deviation in individual pixels, it will lead to a large d. The normalized average absolute distance measurement value r is more sensitive to reflect the small errors of most points. The signal-to-noise ratio is a measure of the ratio of the music element signal to the noise signal, often expressed in decibels.

3.3. Numerical Super-Resolution Reconstruction. In order to obtain high-resolution musical elements, more than 2,000 independent musical elements must be arranged on the ring sensor, which increases the difficulty of data processing and the complexity of system control. In contrast, the linear array has been widely used in the field of ultrasound imaging; its technology is mature; the processing is simple; the cost is low; and it is easy to integrate into the ultrasound tomography system. However, due to the limitation of the transmitting aperture and the limited receiving angle of the ultrasonic signal by the linear array, the tomographic

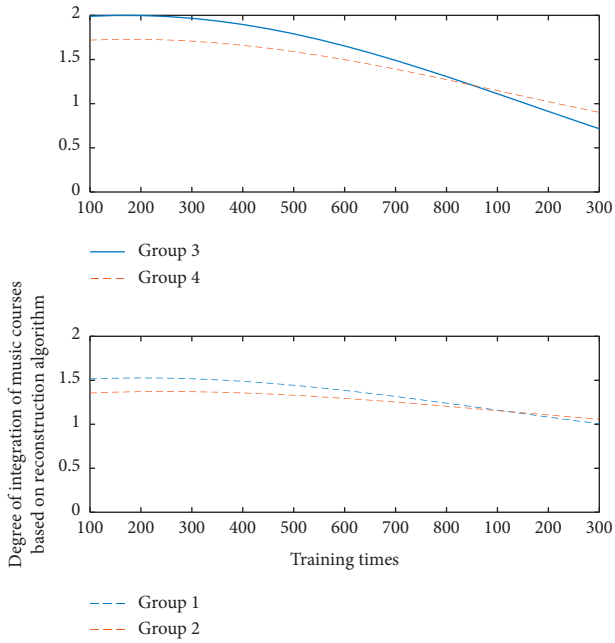

Figure 1: The distribution of the music curriculum integration simulation data test.

reconstruction of the cross-sectional image of the structure cannot be completed in all directions. The parallel beam filtered back-projection algorithm needs the projection data of all parallel beams at all different distances from the symmetry center at all angles from 0 to 180, that is, the projection data of all rays passing through the area to be measured. Although it is impossible to collect projection ray data at every angle and every distance through discretization, the quality of musical elements can be guaranteed by narrowing the sampling interval.

$$\frac{x(p(t,x-1))}{x(p(t))}+\frac{y(p(t,x-1))}{y(p(t))}+\frac{z(p(t,x-1))}{z(p(t))}=0. \quad (5)$$

Therefore, this method has high requirements for the completeness of the collected data. At the same time, because its core algorithm is an integral process, the algorithm complexity is not high, and the running speed is relatively fast. The multiresolution analysis method is to decompose the original music elements, obtain the detailed information on the music elements at different resolutions, and reflect the local characteristics and physical structure of the music elements through the detailed information of different resolutions. The multiresolution analysis algorithm decomposes the original music elements into music element signals of different resolutions, performs fusion processing at different resolutions, and finally inversely transforms and reconstructs the fusion result music elements. The fusion rule is the focus of the current multiscale analysis algorithm. There are two types of fusion rules: pixel-based and region-based. The pixel-based fusion rule determines the value according to the transformation coefficient of the corresponding position. The region-based fusion rule mainly changes the position according to the original music element.

$$\begin{cases} W\{(1-x)(1-y)\}=1, \\ W\{\text{margin}-\text{margout}\}=0. \end{cases} \quad (6)$$

The corresponding transform is determined by performing arithmetic operations. An independent variable increases with the number of iterations, and both the threshold size and the error of the reconstructed signal are nonlinearly decreasing functions. When the error of the reconstructed signal reaches a certain threshold value, the corresponding threshold value is the required threshold value. The advantage is that the calculation time is reduced and the efficiency of the algorithm is improved. Experiments show that the threshold obtained by the adaptive method is approximately equal to the empirical threshold, which verifies the IF accuracy of the algorithm.

The symmetrical diameter of these parallel rays needs to be found, onto which the musical elements on one side are projected. Since the central angle of each musical element in Figure 2 can be obtained by calculation, the position of this musical element on this diameter can also be easily obtained. Then we divide the length of the diameter into 185 equal parts and use the cubic spline interpolation method to obtain new projection data according to the previous 128 projection data. When the number of projection angles is 30, the quality of music elements is extremely poor; the resolution is extremely low; and the tissues are completely indistinguishable; when the number of projection angles is 90, the quality of music elements is significantly higher than when the number of projection angles is 30. However, the three adjacent structures below are turbid and indistinguishable, and the entire music element has serious stripe artifacts; when the number of projection angles is 180, the music element is better recognizable. A clearer distinction is obtained; there are only tiny artifacts in the entire music element; and the overall imaging effect is better.

3.4. Algorithm Advanced Iterative Reconstruction. The algorithm will generate errors in the process of use, such as the inherent error of the algorithm itself, the grid processing of the imaging area, the accuracy of the data filling operation, the error of the interpolation operation, and so on. Some of the errors can be reduced by optimizing the system structure and so on. For the annular array, in order to improve the system accuracy, the methods that can be used include increasing the number of probes and increasing the imaging angle; for the triangular array, because the imaging angle is fixed, the method to improve the system accuracy is mainly to increase the number of probes. This paper then establishes the observation model of super-resolution music element imaging; introduces the principle, classification, and specific methods of music element registration in detail; and conducts image registration and Fourier music based on music element grayscale on the MATLAB 6.1 platform.

$$\prod z(s,t^*)\{(1-t)(1+t)\}-\prod z(s^*,t)\{(1-s)(1+s)\}=0. \quad (7)$$

Experiments were carried out on the element registration method, and the advantages and disadvantages of the two methods were compared and analyzed. Three

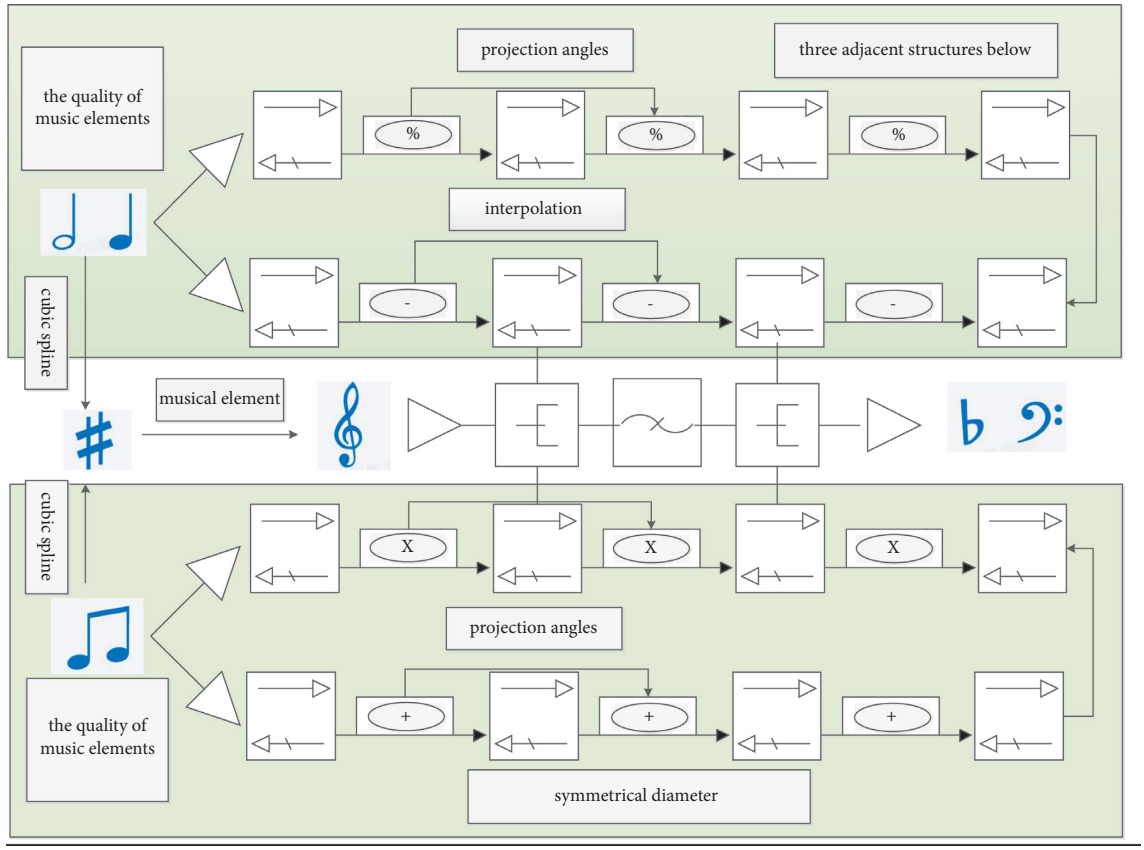

Figure 2: Schematic diagram of inverse transformation of music curriculum elements.

commonly used interpolation methods (nearest-neighbor interpolation, linear interpolation, and cubic interpolation) are discussed, and the reconstruction results of their corresponding MATLAB simulations are compared, and it is concluded that the quality of the reconstruction results obtained by the cubic interpolation method is better than the other two methods. The idea of a music element fusion algorithm based on independent component analysis (ICA) is to transform the original music elements by training the ICA base to obtain the transformed coefficients and then adopt the fusion rules to fuse the transformed coefficients. The coefficients are inversely transformed to reconstruct the fusion result musical elements. The description and implementation steps of the music element fusion algorithm based on the ICA method are shown in the algorithm.

$$\begin{cases} \bigcap_{i=2,j=2}^{i+j} \max(i-2, j-2) + \max(i, j) = 0, \\ \bigcap_{i=1,j=1}^{i+j} \max(i-1, j-1) + \max(i, j) = 1. \end{cases} \tag{8}$$

In a parallel projection with an angle of it, the musical element numbers between the musical elements at both ends of the projection path move closer to the middle from both sides, reducing two musical elements each time, and the obtained rays are all parallel to each other. The norm cannot maintain the sparsity of the original signal, and the sparsity of the reconstructed signal cannot reach the sparsity of the true noise-free signal, so the coefficient amplitude of the reconstructed signal cannot reach the coefficient amplitude of the original signal.

From the general view of Figure 3, the calculation efficiency of the projection matrix based on ray drive is much higher. And when there are more voxels in the reconstruction region, this advantage is more obvious. Therefore, the ray-driven SART algorithm is more suitable for the subsequent higher-resolution reconstruction scenes. Therefore, in the following experiments, the SART reconstruction experiments are carried out with the projection matrix calculated by the ray-driven calculation. After the projection matrix is calculated, the reconstruction can be performed according to the projection matrix of each projection angle. The flow chart of one iteration of cone-beam SART reconstruction is shown in the text. After one iteration is completed, the next iteration is performed with the result of one iteration as the initial value, until the number of iterations reaches the preset value. The steps of the SIRT algorithm are roughly similar to the SART algorithm, except that the calculation of the correction value in the SART algorithm involves the multiplication and division of some constant terms. In this algorithm, the correction value of each pixel is the accumulation of the correction

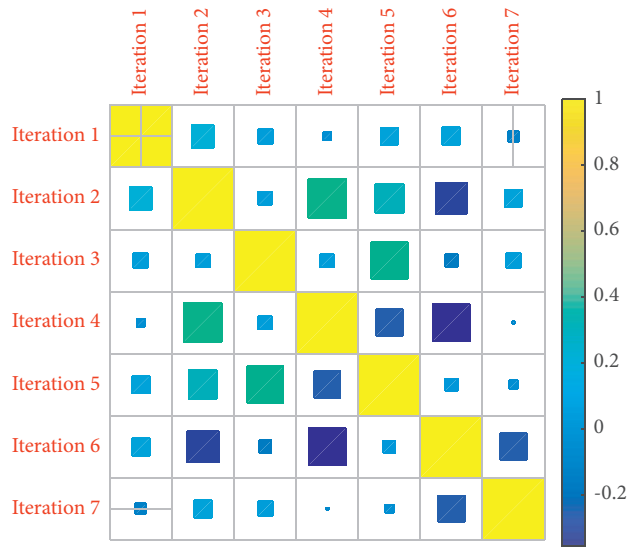

Figure 3: Matrix calculation efficiency distribution of advanced iterative reconstruction algorithm.

values of all rays passing through the pixel point; some random errors can be averaged; and the influence of noise in the measurement data on the final solution can be effectively avoided based on the least-squares method.

It can be seen from Table 2 that the reconstruction speed is very slow, and as the resolution of the reconstruction area and the number of projected rays increase, the reconstruction time increases exponentially and the memory space required for the reconstruction also increases greatly. In practical applications, when the resolution of the projection equipment is high or the reconstruction area requires a high resolution, iterative reconstruction algorithms such as SART will not be able to meet the needs of practical engineering applications. Since the reconstructed object is usually located in the area with the origin as the center and the annular radius of the ultrasound probe as the radius, this area is usually defined as the imaging area, and the space outside the circle is discarded. The algorithm for solving the coefficient matrix is as follows: first, we convert the coordinates of the transmitted and received musical elements into the coordinates of the square area to be measured. According to the different directions of the ray, it is divided into four cases (relative to the coordinate system) in the simulation. The four cases are (1) the ray is horizontal; (2) the ray is perpendicular to the x-axis; (3) the slope is greater than 0; and (4) the slope is less than 0.

Table 2: Example analysis of measurement data.

	Complex ratio 1	Complex ratio 2	Complex ratio 3
Information degree	2.77	2.87	2.97
Relative error	1.84	1.9	1.96
Maximum correlation	0.91	0.93	0.95
Balance error	0.02	0.04	0.06
Average correlation	0.95	1.01	1.07
Minimum correlation	1.88	1.98	2.08
Confidence error	2.81	2.95	3.09

4. Music Curriculum Integration and Reconstruction Model Construction Based on Advanced Iterative Reconstruction Algorithm

4.1. Course Iterative Measurement Matrix Optimization. First, a Gaussian random matrix with dimension $M \times N = 100 \times 256$ is generated as a measurement matrix, and then the sparsity seven is continuously changed to randomly generate a sparse signal of length $N = 256$. The number of iterations is the same as the sparsity k. Each sparsity degree repeats the experiment 1,000 times under k. It can be seen that the reason why these four algorithms show different characteristics and performance is because of the different methods of selecting atoms and the conditions for stopping iteration. This section takes the previous experiments as the research basis and analyzes and compares the reconstruction performance of several algorithms from the four aspects of reconstruction power, relative error, reconstruction time and peak signal-to-noise ratio (PSNR), and further draws the differences between them.

$$\begin{bmatrix} T_{ij} & 1 \\ -1 & -T_{ij} \end{bmatrix} \times \begin{bmatrix} Y_{ij} & \log a \\ -\log a & -Y_{ij} \end{bmatrix} - \begin{bmatrix} e(i,j) & 0 \\ 0 & e(i,j) \end{bmatrix} = 0. \quad (9)$$

In practical engineering applications, the sparsity k of the signal is often not known in advance, and k needs to be estimated, which greatly restricts the practical application of these algorithms. If the estimation of k is too small, it will reduce the reconstruction accuracy of the algorithm and even make it difficult for the algorithm to converge; if the estimation of k is too large, the reconstruction quality and robustness of the algorithm will be poor and even lead to the reconstructed signal distortion occurs. Based on this, in the following chapters, this paper focuses on the algorithm that

can reconstruct blind sparse (i.e., unknown sparsity) signals with high probability. Since the music signal is an unstable random signal and the signal is weak, it is easy to be interfered by the signals during the acquisition process, as well as the noise of the external power supply, the noise of the instrument itself, space radio frequency interference, and other noises.

$$\frac{\sum Y\lfloor i|i=0,1,2,3,j-1,j\rfloor_i}{\sum_{i=1}^{N} Y\cdot X_i}-\frac{\sum Y\left[j|j=0,1,2,3,i-1,i\right]_j}{\sum_{j=1}^{N} Y/X_j}=0. \tag{10}$$

Therefore, the elimination of noise is crucial. Discrete wavelet transform (DWT) is an effective time-frequency analysis method, which can effectively extract the characteristics of signals. Because discrete wavelet transform (DWT) has a good performance in discrete music signal analysis, wavelet transform is generally used to preprocess the collected music signal in the research to remove noise and baseline drift. The first-order difference can reflect the change trend and speed of the signal, and it is used to detect the local extreme point of the signal, and the second-order difference can detect the local inflection point of the signal. Table 3 includes features such as mean, median, standard deviation, minimum, maximum, difference between minimum and maximum, ratio of minimum, and ratio of maximum.

The discrete wavelet transform can decompose the signal into different scales through low- and high-pass filtering. After high-pass filtering, the detail coefficient D is obtained, and after low-pass filtering, the approximate coefficient A is obtained. The consistent Daubechies 5 wavelet is used as the basis function to decompose the denoised EMG signal layer by layer. Among them, the approximate coefficient A can continue to be subjected to high- and low-pass filtering and then decomposed to the next layer to get a more original feature combination including statistics such as median, mean, standard deviation, range, and locally maximized ratios. In the frequency domain, the spectral power of the respiratory signal is in the range of 0–0.1 Hz, 0.1–0.2 Hz, 0.2–0.3 Hz, and 0–0.4 Hz. The energy ratio includes the energy ratio of the low frequency band (0.05–0.25 Hz) and the energy ratio of the high frequency band (0.25–5 Hz).

4.2. Evaluation Criteria for Advanced Iterative Algorithms. Feature selection is an important dimension reduction technique in the evaluation of algorithm pattern recognition. It is used for data vector spaces or high-dimensional data sets containing redundant features. On the premise of not affecting the calculation effect, the feature set is defined. It eliminates irrelevant and redundant information, effectively reduces the data dimension of original features, reduces computational cost and storage space, and speeds up the data mining process. In addition, the performance of the post-classification learning algorithm is improved, the accuracy of emotion recognition is improved, and the performance of the model is improved. It also borrows a back-off screening strategy, that is, each cycle selects k (the sparsity of the signal) atoms with the greatest correlation with the signal residual into the atomic set, ensuring that the number of atoms in the candidate set does not exceed 2 at most.

$$\begin{cases} \lim \sum_{n} z_{ij}(m,n)\cdot z_{ij}(i+m,j+n)=1, \\ \lim \sum_{m}\sum_{n} z_{ij}(m,n)=1. \end{cases} \tag{11}$$

At the same time, some unsuitable atoms are eliminated. After the iteration is completed, seven optimal atoms are finally selected to solve the best approximate solution of the original signal. This idea of back-screening atoms can greatly reduce the error caused by the ROMP algorithm processing multiple atoms in one iteration by selecting and eliminating atoms multiple times. It represents the high-resolution full-color music element; m, n are the high and low frequency components of low-resolution multispectral music elements, respectively; and R, G, and screen represent the R, G, and B components of the fused music element, respectively. After fusion, in order to be consistent with the grayscale of the multispectral music elements, it is necessary to do grayscale stretching of the R, G, and B component music elements. This algorithm is suitable for information fusion of music elements collected by different sensors. Brovey transform can only process true color or pseudocolor music elements in three bands and is not suitable for the fusion of panchromatic music elements and multispectral music elements with inconsistent spectral ranges.

$$\begin{aligned} &\left[I\left(x_1,x_2,x_3\right),J\left(x_1,x_2,x_3\right),K\left(x_1,x_2,x_3\right)\right]\times P \\ &=\left\langle \begin{matrix} \max(i,j,k|i+j+k<1), \\ \min(1,x). \end{matrix}\right. \end{aligned} \tag{12}$$

According to the specific personalized music recommendation scenarios, a relatively complete and objective music emotion database is established, and music signals are collected, and then the conventional features and nonlinear features are extracted from these music signals, and the music signal feature set is obtained. The optimal feature set is established through feature selection and feature dimensionality reduction, and the pattern recognition of various machine learning algorithms is carried out on the characteristics of music objects and music signals. A music emotion cognition model based on the NuSVR algorithm is proposed and applied to a personalized music emotion recommendation system. It provides a case reference for researchers designing products or systems based on music signals.

The improved algorithm shown in Figure 4 inherits the advantages of the SAMP algorithm, organically combines the optimized regularization method with the backtracking idea, optimizes the atomic matching strategy, and further improves the accuracy of atomic selection and self-adaptive, thereby reducing the reconstruction error and completing the effective recovery of blind sparse signals. The simulation results show that the improved algorithm is better than the original algorithm in terms of reconstruction success rate

Table 3: Description of the advanced iterative reconstruction algorithm.

Code number	Reconstruction algorithm description	Content text
1	$\iint \sin\theta$ dimension	Case "+":cout << x<<"+"<<y<<"="<<$x+y$ << endl
2	The respiration rate Q(on)	For(int $i=1$; $i \le 10$; i++)
3	The elimination of $t-1$	Case "−":cout << x<<"−"<<y<<"="<<x-y << endl
4	$3\pi d(I, J)$ includes features	For(float $x1=0$; $x1 \le 1.0+0.1/2$; $x1=x1+0.1$)
5	Respiration amplitude Gau(ss)	Case "$*$":cout << x<<"$*$"<<y<<"="<<$x * y$ << endl
6	Discrete wavelet $q(i)$	Cout<<"sizeof(st)="<<sizeof(st)<<endl
7	Discrete music signal	Cout<<"sizeof(student1)="<<sizeof(student1)<<endl
8	The local inflection X(on)	If ($n \ge 0$&&; $n \le 100$ &&n%2==0)
9	It is used to t^2	Cout<<"n="<<n << endl
10	Such as mean max$(t, t-1)$	Cout<<"sum="<<sum << endl
11	Matrix(on) can continue	Cout<<"The "<<n<<" is out of range!"<<endl
12	Ratio of minimum a^2+b^2	Cout<<"i"<<i<<"$*$"<<j<<"="<<$i*j$
13	The approximate $Z'(q(i))$	L2: cout<<"sum="<<sum << endl
14	Coefficient min$(t, t-1)$	Cout<<a[0]<<a [1]<<a [2]<<a [3]<<a [4]<<endl
15	Difference between minimum $3\pi d$	Cout<<"sizeof(int)="<<sizeof(int)<<endl
16	High-pass filtering	Cout<<"sizeof(float)="<<sizeof(float)<<endl
17	The signal into Matrix(ide)	Cout<<"sizeof(double)="<<sizeof(double)<<endl
18	The consistent $Z(i)$	Cout<<"sizeof(char)="<<sizeof(char)<<endl

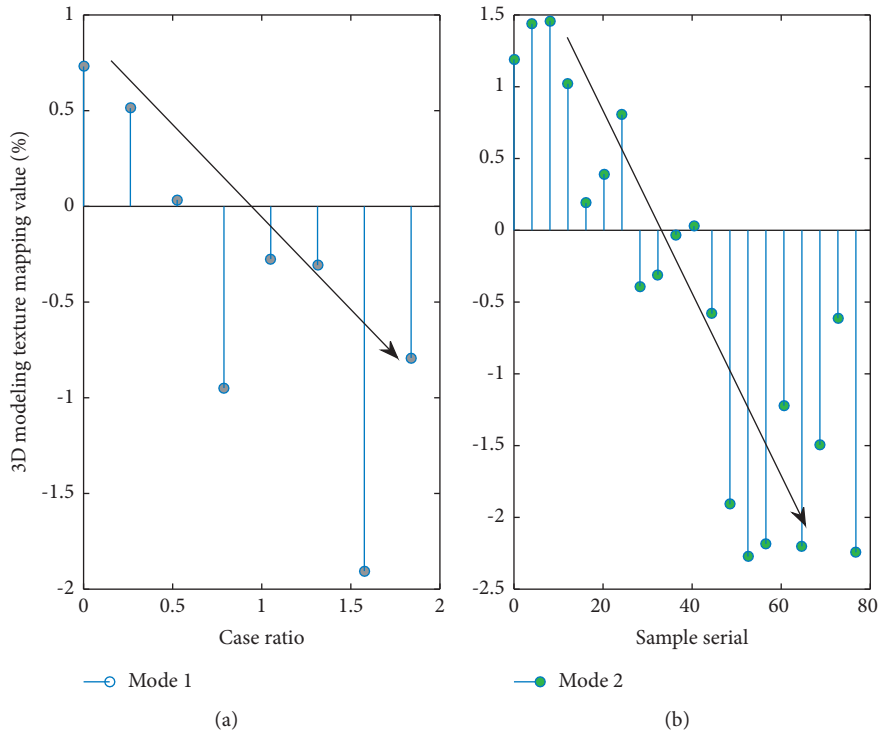

Figure 4: Design distribution of music signal course system.

and reconstruction quality, and the operation time is also slightly lower than the original algorithm due to the regularization process. The first problem is that $R=$ IV cannot be assumed. In fact, in most applications, it is redundant IV. Sometimes, it is possible to force $R=$ IV by using an interpolation algorithm on the projected musical elements. The least squares method can be used to solve linear equations when brother > IV, but the computational complexity is greater when IV is relatively large. In a more general case, the equation Wz $= p$ has many sets of solutions when IV $> R$. So the goal of the ART reconstruction algorithm is to obtain the closest estimate of the reconstructed area by projecting musical elements.

4.3. Music Curriculum Integration Factor Analysis. The joint iteration method (SIRT) is a parallel computing form of the ART algorithm. In this method, all the pixels of a certain projection p are calculated first, and then the voxels of the entire reconstruction area are updated. Before the updated value is added to the voxel value, it needs to be weighted and normalized with the weighted value. Therefore, the SIRT

algorithm converges slowly and is not widely used. The SIRT algorithm is proposed to make the reconstruction insensitive to measurement errors. As mentioned in the previous section, the ray sum (or ray projection) of only one ray is used in each iteration of the AI staring algorithm. If this ray projection contains errors, then the resulting solution also introduces errors. In the method based on compressive sensing, sampling and compression are carried out at the same time, and the original signal x is directly nonlinearly projected to obtain M, and M contains enough reconstruction information.

$$\begin{cases} \langle \cos\left(Z_j(i,j) + Z_j(i-1,j-1)\right)\Big| = \langle \cos(i+j)|, \\ \langle \sin\left(Z_j(i,j) + Z_j(i-1,j-1)\right)\Big| = \langle \sin(i+j)|. \end{cases} \tag{13}$$

At present, the super-resolution reconstruction technology of music elements is divided into two categories based on the spatial domain and the frequency domain. The frequency domain-based super-resolution reconstruction algorithm is mainly based on the shift characteristics of the Fourier transform. The idea of the frequency-domain music element super-resolution reconstruction algorithm is to perform discrete Fourier DFT transform on the registered undersampled music elements, according to the spectral aliasing relationship between DFT and CFT, the relationship between the undersampled music element and the super-resolution reconstructed music element is solved, and the super-resolution music element is reconstructed according to the registration parameters and the existing undersampled music element signal data. Similarly, in order to describe the reconstruction performance of the CoSaMP algorithm more vividly, this paper uses the MATLAB 7.10.0 program to reconstruct the one-dimensional sparse signal. Under the condition that the number of measurements M is fixed, the simulation in Figure 5 shows the reconstruction.

The algorithm can accurately restore all sensing matrices that satisfy the RIP characteristics and signals with known sparsity, and the reconstruction time is very short. The core idea is: for the reconstruction of the July 1 sparse signal, the ROMP algorithm uses the inner product method to select atoms for the first time. The correlation coefficient is the signal residual and the absolute value of the inner product of each column vector of the sensing matrix. Then select the k atoms with the largest amplitude from u and put them into the candidate set A; secondly, according to the regularization method in it, the atoms corresponding to A are processed, and the group with the largest energy is selected. Enter the set A0 to complete the secondary screening of atoms; finally, complete the update of the support set F, the least squares method obtains the approximate solution of the original signal, and the residual is updated. The local Fourier matrix is obtained by randomly selecting M rows from the Fourier matrix and then uniting the columns.

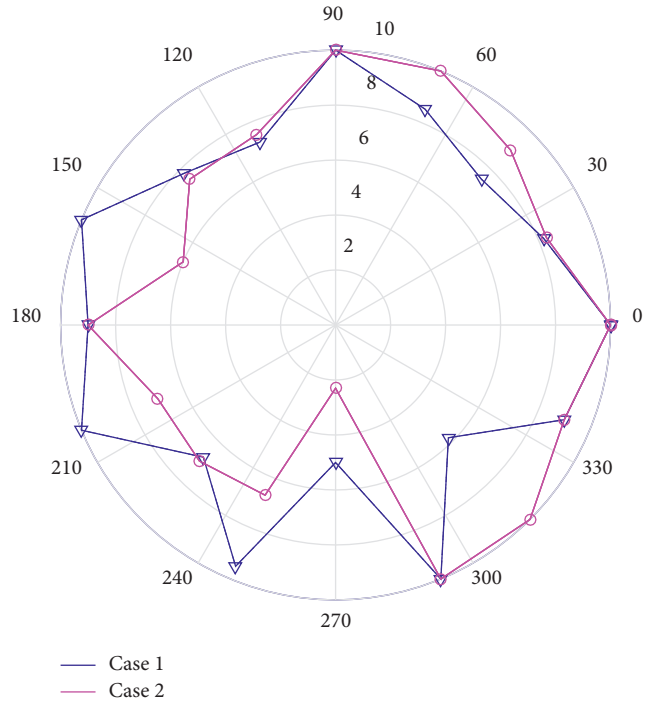

Figure 5: Sparsity representation of advanced iterative gradient algorithm.

5. Application and Analysis of Music Course Integration and Reconstruction Model Based on Advanced Iterative Reconstruction Algorithm

5.1. Iterative Reconstruction Algorithm Data Preprocessing. In this chapter, the CUDA development environment will be used to accelerate the GPU acceleration of the SART reconstruction algorithm after a certain optimization so that the iterative reconstruction using the SART algorithm has the feasibility of a practical application. In this chapter, the basic concepts of the CUDA development environment are first introduced, and then the SART algorithm is improved to meet the development requirements of CUDA programs. Finally, the serial CPU code is changed to parallel CUDA code, and according to some characteristics of CUDA, to optimize the task division of parallel computing to achieve the greatest possible speedup. In each iteration, the atoms most relevant to the current signal or the iterative residual are selected from the atomic library (i.e., the measurement matrix) using the correlation principle for sparse approximation so that after several iterations, the original sparse signal is approximately linearly represented.

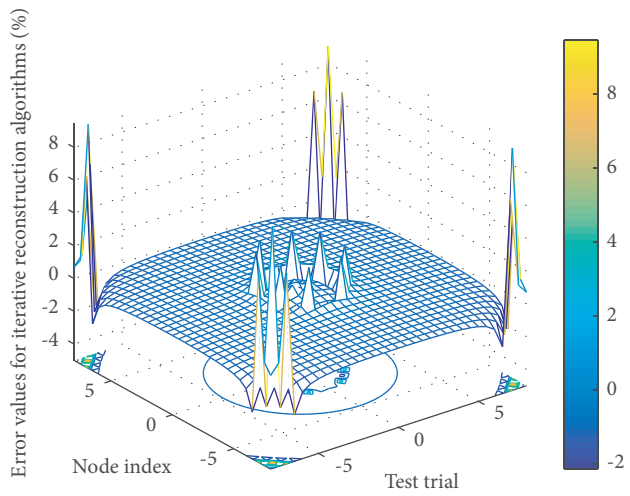

Figure 6: 3D distribution of signal error of advanced iterative reconstruction algorithm.

When the sampling rate of the OMP algorithm is small, the operation time is short, but the relative reconstruction error is large, and when the sampling rate is large, the reconstruction relative error is small, but the operation time is long. In general, the OMP algorithm can reconstruct the original music elements better when the sampling rate is different. However, the OMP algorithm also has two defects: (1) the computational complexity is greatly increased due to the introduction of the most d multiplication and (2) only one atom is selected for each iteration to update the support set, resulting in a long-running time, which makes the OMP algorithm very limited in the application of some large-scale signal reconstruction.

Taking the projection value p as the initial value of back projection, in the seventh + 1 iteration, Figure 6 uses the seventh iteration result $z7$ plus the correction value to obtain $z7 + l$, the correction value, and the seventh estimated error vector, so the correction value for each voxel is the sum of the error values for all rays passing through that voxel, not just one ray. Therefore, the correction process of SIRT is called point-by-point correction. This is the biggest difference from the ART algorithm and the fundamental reason why the SIRT algorithm can suppress noise: some random errors are averaged out by the common contribution of all rays passing through the voxel. After one iteration, all voxels are updated at one time, which can effectively eliminate stripe artifacts. However, as shown in the previous chapter, the problem with the SIRT algorithm is that the convergence speed is slow, and more iterations are required to achieve better results.

5.2. Realization of Music Course Integration Reconstruction Simulation. A CUDA program consists of host code and device code. The NVIDIA C compiler (nvcc) separates the two parts of the code during the compilation phase. The host-side code is ordinary ANIS C code, which can be compiled into ordinary host-side threads by a standard C compiler. The device-side code written in the ANIS C extension tag requires special processing. These codes mainly define the functions of data-parallel computing and related data structures, and these functions are called seven. The device code is further compiled by nvcc into code executable on the GPU. The runtime of a CUDA program includes several different operating states: executing on the host side (such as CPU) and executing on the device side (such as GPU). A system can contain one host and several devices. The essence is a greedy iterative algorithm, that is, in each iteration, a certain atomic matching criterion is used to select one or more atoms most relevant to the signal to gradually approximate the sparse solution of the signal and realize the final reconstruction of the original signal. It can be seen that in this type of algorithm, how to select the appropriate atom is very critical. If the appropriate atom can be selected, the original signal can be accurately reconstructed with a high probability.

$$\begin{bmatrix} I(x_1) \times y(x_1), I(x_2) \times y(x_2), I(x_3) \\ \times y(x_3), \ldots, I(x_{n-1}) \times y(x_{n-1}), I(x_n) \times y(x_n) \end{bmatrix} = I \times Y. \tag{14}$$

Each pixel value in itself contributes to the correction value of each voxel, and the updated value of each voxel is obtained by accumulating these contributions on each voxel. If the correction terms are simply added, the noise that may exist in the projected musical elements will be added to the reconstructed musical elements to produce artifacts, so weighting needs to be performed when updating. It can be seen that the convergence speed of ART and SART reconstruction is faster, and the optimal solution can basically be obtained in 5 iterations, while the convergence speed of the sIIu reconstruction algorithm is slower, and it still needs 10 when using a larger relaxation coefficient. It takes more than one iterations to converge, which also proves the above theoretical research.

At the same time, as shown in the text, with the increase in the number of iterations, the reconstruction result of the ART reconstruction algorithm gradually deviates with the increase in the number of iterations after reaching the optimal result. The SIRT reconstruction algorithm has a slower convergence rate. After reaching the optimal solution, the reconstruction results in Figure 7 do not significantly deteriorate with the increase of the number of iterations. The SART reconstruction algorithm combines the advantages of the above two algorithms, which not only can converge quickly to obtain the optimal solution but also can reconstruct the results after convergence without deteriorating the quality with the increase of the number of iterations.

In the signal decomposition process, the denoised original signal is first filtered into high pass and low pass, respectively, and then the corresponding coefficients of the detailed coefficients of the high- and low-pass signals are used as signal features. Then, the DSP and DSAMP algorithms are applied to the reconstruction of one-dimensional time-domain signals and two-dimensional music elements, and compared with SP and SAMP, respectively; the simulation results show that the two improved algorithms DSP

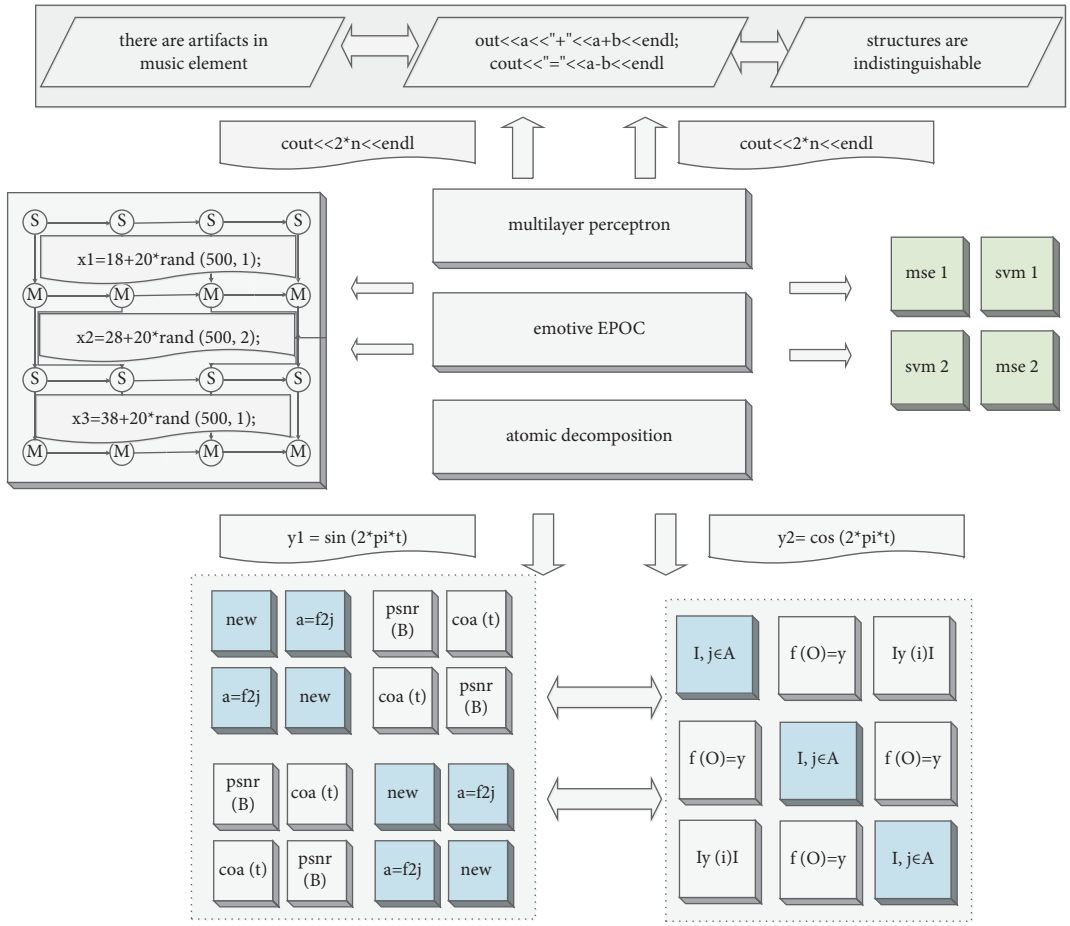

Figure 7: Signal decomposition process of advanced iterative reconstruction algorithm.

and DSAMP can improve the reconstruction quality of sparse signals. Both are better than the original algorithm, which further verifies that the dice coefficient atom matching criterion can better select the atoms most related to the residual from the sparse dictionary and has better reconstruction quality.

$$\begin{vmatrix} \sqrt{f\left(t-t^2\right)} & \max\left(t,t-1\right) & 1 \\ \min\left(t,t-1\right) & \sqrt{f\left(t-t^2-1\right)} & \min\left(t,t-1\right) \\ 1 & \max\left(t,t-1\right) & \sqrt{f\left(t-t^2+1\right)} \end{vmatrix} = \begin{vmatrix} \log t & 1 & 0 \\ 1 & \log t+1 & 1 \\ 0 & 1 & \log t+n \end{vmatrix}. \quad (15)$$

Each decomposition level produces different coefficients. The mechanism of decomposition is that the sampling rate of each layer is reduced by half so that the value of the coefficient is different between layers 1 and 6, but the difference between layers 1 and 6 changes gradually, so in this experiment, only the coefficients of layers 1 and 6 are selected to represent signal information. After DwT processing, we first use statistical analysis methods to analyze the raw signals, including the detailed signals of layers 1 and 6 (DET1 and DET 6), the approximate signals of layers 1 and 6 (APP1 and APP6), and the coefficients of DET1, DET6, and APP1. The statistical eigenvalues obtained from the original signal and the decomposed signal include the maximum value.

5.3. Example Application and Analysis. Based on the feature database, we analyzed and compared the recognition of LR, RR, SVR (1inear kernel), SVR (rbf kernel), SVR (poly kernel), MLP, and NuSVR and other regression algorithms. NuSVR achieved the best recognition effect. In all data fusion comparisons, the data set with all features (all musical features and all musical features) performed best in modeling. In the second case, we used multilayer perceptron, Kstar, and SVM to model and analyze the music diameter change data and found that SVM achieved the best results. In case 3, we used repeated measures ANOVA and correlation analysis and concluded that music signals such as electrical skin can be used as objective indicators of user emotion measurement. Finally, we present three cases

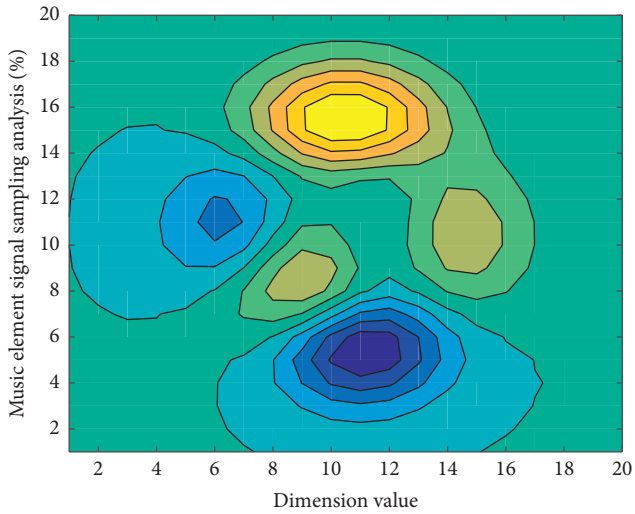

Figure 8: High-dimensional music element signal sampling analysis.

of music signal-based product or system design and user experience evaluation.

$$\begin{cases} \iint T(i,j)\mathrm{d}i\mathrm{d}j = \lim\left[i,j\middle|\left(P_i(i,j)\right)^2 + \left(P_i(i,j)\right)^2\right]^{1/3}, \\ \iint S(i,j)\mathrm{d}i\mathrm{d}j = \lim\left[i,j\middle|\left(P_i(i,j)\right)^2 - \left(P_i(i,j)\right)^2\right]^{1/3}. \end{cases} \tag{16}$$

MPl50 series music signal amplifier modules are single-channel, differential input, linear amplifier modules with adjustable gain compensation. These modules are used to amplify small voltage signals collected from electrodes or sensors and convert them to output. In addition, in addition to amplifying the signal, MPl50 series modules can also filter or convert the data into the required form. It will be read in the shared memory at the beginning of each 6fDc operation. When calculating the rotation matrix later, the speed of reading the data in the shared memory directly is greatly improved compared to reading from the global memory (G10bal Memo). Therefore, the basis for calculating the rotation matrix task division is the size of each 620c seven shared memory. The operation of rotating the volume data through the rotation matrix is similar to the above process, but it is not necessary to read the content of the rotation matrix into the shared memory, because the data is only used once during the rotation process, and there is no need to read it multiple times. So this operation is meaningless.

At present, the research of transform basis mainly focuses on the intersection basis, but in the face of some more complex signals, such as high-dimensional music element signals and sound signals, it is difficult to make them very sparse with the intersection basis. Figure 8 is more efficient to sparsely express complex signals with atoms in an overcomplete redundant dictionary. However, there are too many atoms in the dictionary, and musical elements with complex geometric features and sound signals with complex compositions must be represented by many atoms. In this experiment, we still use musical emotional clips as stimulus materials.

$$\begin{cases} \mathrm{Matrix}(ide) = \beta \times X(\mathrm{on}) \times Y(\mathrm{off}) \times \left(\dfrac{\lambda \times \alpha}{3\pi d(I,J)}\right)^2, \\ \mathrm{Matrix}(on) = X(\mathrm{coordinate}) \times Y(\mathrm{coordinate}). \end{cases} \tag{17}$$

Then select a 10 s piece of music with the main emotion to generate a piece of music. These extracted fragments are saved as WAV format; the sampling rate is 16 KHz, in order to retain the maximum music information to ensure the best listening experience. The 360 pieces of music are divided into 6 groups. In order to balance the emotions of the 4 quadrants to the greatest extent, each group contains 15 happy pieces (high-valence, high-arousal music, such as Spring Festival Overture), 15 calm music fragments (high-valence, low-arousal music, such as Jasmine), 15 sad music fragments (low-valence, low-arousal music, such as Erquan Yingyue), and 15 tense music fragments (low-valence, high-arousal music, such as music describing war).

6. Conclusion

In this paper, by comparing the accuracy with the other two algorithms on the basis of controlling the sparsity of the integrated data of music courses as a variable, the research on the three algorithms shows that the joint algebraic reconstruction algorithm (SART) has the advantages of both reconstruction quality and reconstruction speed. There are certain advantages, and the calculation methods of projection matrix based on ray-driven and voxel-driven are discussed and their influence on SART reconstruction results. Finally, the SART reconstruction algorithm based on ray-driven projection is selected for further optimization. In this paper, the rotation of the projection system is mapped to the rotation of the reconstruction area data, which avoids the calculation of the projection matrix at each angle. Furthermore, by using the symmetry of the projection system, it is only necessary to calculate the projection matrix corresponding to 1/4 of the number of rays, and the remaining 3/4 can be calculated by symmetry. After these improvements, the SART algorithm has a certain improvement in the reconstruction speed. At the same time, using the super-resolution reconstruction algorithm proposed in this paper, the super-resolution reconstruction of a single music element is realized, and a good reconstruction effect is achieved. Finally, a single-frame music element super-resolution reconstruction algorithm based on advanced iterative reconstruction and learning dictionary is proposed, and the self-similarity of music elements and the training method of learning dictionary are described. The improved local Hadamard matrix is selected as the measurement matrix to ensure that the reconstruction of musical elements complies with the RIP criterion of advanced iterative reconstruction theory; the super-resolution reconstruction of single musical elements is achieved through an iterative algorithm. Experiments show that the reconstructed music elements obtained by the advanced iterative gradient reconstruction algorithm have better visual effects, and the

PSNR value is improved compared with the bilinear interpolation and SRSR algorithms.

Data Availability

The data used to support the findings of this study are available from the corresponding author upon request.

Conflicts of Interest

The author declares that there are no conflicts of interest.

Acknowledgments

This work was supported by the College of Music and Dance, Chengdu University.

References

[1] Y. Tian, X. Chai, Z. Gan, Y. Lu, Y. Zhang, and S. Song, "SWDGAN: GAN-based sampling and whole image denoising network for compressed sensing image reconstruction," *Journal of Electronic Imaging*, vol. 30, no. 6, Article ID 63017, 2021.

[2] H. Akbari, B. Khalighinejad, J. L. Herrero, A. D. Mehta, and N. Mesgarani, "Towards reconstructing intelligible speech from the human auditory cortex," *Scientific Reports*, vol. 9, no. 1, pp. 874–912, 2019, doi: 10.1038/s41598-018-37359-z.

[3] Z. Zheng, Y. Zheng, W.-Q. Wang, and H. Zhang, "Covariance matrix reconstruction with interference steering vector and power estimation for robust adaptive beamforming," *IEEE Transactions on Vehicular Technology*, vol. 67, no. 9, pp. 8495–8503, 2018.

[4] R. Orjesek, R. Jarina, and M. Chmulik, "End-to-end music emotion variation detection using iteratively reconstructed deep features," *Multimedia Tools and Applications*, vol. 81, pp. 11–15, 2022.

[5] H. Wang, H. Zhang, and Q. Ma, "Sparse spectrum fitting algorithm using signal covariance matrix reconstruction and weighted sparse constraint," *Multidimensional Systems and Signal Processing*, pp. 10-11, 2022, doi: 10.1007/s11045-021-00811-x.

[6] T. Konno, K. Nishida, K. Itoyama, and K. Nakadai, "Audio-visual 3D reconstruction framework for dynamic scenes," in *Proceedings of the 2020 IEEE/SICE International Symposium on System Integration (SII)*, pp. 802–807, IEEE, Honolulu, HI, USA, January 2020.

[7] H. Liu, C. Tan, S. Zhao, and F. Dong, "Nonlinear ultrasonic transmissive tomography for low-contrast biphasic medium imaging using continuous-wave excitation," *IEEE Transactions on Industrial Electronics*, vol. 67, no. 10, pp. 8878–8888, 2019.

[8] V. Upadhyaya, G. Sharma, A. Kumar, S. Vyas, and M. Salim, "Quality parameter index estimation for compressive sensing based sparse audio signal reconstruction," *IOP Conference Series: Materials Science and Engineering*, IOP Publishing, vol. 1119, no. 1, Article ID 12005, 2021.

[9] M. Luo, X. Yang, X. Huang et al., "Self context and shape prior for sensorless freehand 3D ultrasound reconstruction," in *Proceedings of the International Conference on Medical Image Computing and Computer-Assisted Intervention*, pp. 201–210, Springer, Strasbourg, France, October 2021.

[10] Y. Lai, Y. Xue, C. Y. Côté et al., "Single-shot compressed ultrafast photography in the ultraviolet spectral range," *High-Speed Biomedical Imaging and Spectroscopy VI. International Society for Optics and Photonics*, vol. 11654, Article ID 116540J, 2021.

[11] J. Shen, M. Tao, Q. Qu, D. Tao, and Y. Rui, "Toward efficient indexing structure for scalable content-based music retrieval," *Multimedia Systems*, vol. 25, no. 6, pp. 639–653, 2019.

[12] C. Li, C. Liu, L. Duan, P. Gao, and K. Zheng, "Reconstruction regularized deep metric learning for multi-label image classification," *IEEE Transactions on Neural Networks and Learning Systems*, vol. 31, no. 7, pp. 2294–2303, 2019.

[13] A. Daneshzadeh and G. Sirrakos, "Restorative justice as a doubled-edged sword: conflating restoration of black youth with transformation of schools," *Taboo: The Journal of Culture and Education*, vol. 17, no. 4, p. 2, 2018.

[14] R. Guarnieri, M. Zhao, G. A. Taberna, M. Ganzetti, S. P. Swinnen, and D. Mantini, "RT-NET: real-time reconstruction of neural activity using high-density electroencephalography," *Neuroinformatics*, vol. 19, no. 2, pp. 251–266, 2021.

[15] K. Wang, D. Niu, L. Sun et al., "Wind power short-term forecasting hybrid model based on CEEMD-SE method," *Processes*, vol. 7, no. 11, p. 843, 2019.

[16] L. Stankovic and M. Brajovic, "Analysis of the reconstruction of sparse signals in the DCT domain applied to audio signals," *IEEE/ACM Transactions on Audio, Speech, and Language Processing*, vol. 26, no. 7, pp. 1220–1235, 2018.

[17] H. H. Dam, S. Y. Low, and S. Nordholm, "Two-level optimization approach with accelerated proximal gradient for objective measures in sparse speech reconstruction," *Journal of Industrial and Management Optimization*, vol. 2, no. 6, pp. 39–43, 2021.

[18] P. A. Gómez, M. Cencini, M. Golbabaee et al., "Rapid three-dimensional multiparametric MRI with quantitative transient-state imaging," *Scientific Reports*, vol. 10, no. 1, Article ID 13769, 2020.

[19] X. Ji, "Reconstruction of multipolar point sources with multi-frequency sparse far field data," *Inverse Problems*, vol. 37, no. 6, Article ID 65015, 2021.

[20] Y. Shi, Z. Rao, C. Wang, Y. Fan, X. Zhang, and M. Wang, "Total variation regularization based on iteratively reweighted least-squares method for electrical resistance tomography," *IEEE Transactions on Instrumentation and Measurement*, vol. 69, no. 6, pp. 3576–3586, 2019.

[21] H. Alkadhi and A. Euler, "The future of computed tomography," *Investigative Radiology*, vol. 55, no. 9, pp. 545–555, 2020.

[22] M. Roohi, J. Mazloum, M.-A. Pourmina, and B. Ghalamkari, "Machine learning approaches for automated stroke detection, segmentation, and classification in microwave brain imaging systems," *Progress In Electromagnetics Research C*, vol. 116, pp. 193–205, 2021.

[23] Y. Xu, "Sparse abundance estimation with low-rank reconstruction for hyperspectral unmixing," *International Journal of Remote Sensing*, vol. 41, no. 17, pp. 6805–6830, 2020.

[24] S. Salehi, M. B. Mashhadi, A. Zaeemzadeh, N. Rahnavard, and R. F. DeMara, "Energy-aware adaptive rate and resolution sampling of spectrally sparse signals leveraging VCMA-MTJ devices," *IEEE Journal on Emerging and Selected Topics in Circuits and Systems*, vol. 8, no. 4, pp. 679–692, 2018.

[25] J. Assländer, M. A. Cloos, F. Knoll, D. K. Sodickson, J. Hennig, and R. Lattanzi, "Low rank alternating direction method of multipliers reconstruction for MR fingerprinting," *Magnetic Resonance in Medicine*, vol. 79, no. 1, pp. 83–96, 2018.